Journal of Power Sources 245 (2014) 594–598

Contents lists available at SciVerse ScienceDirect

Journal of Power Sources

journal homepage: www.elsevier.com/locate/jpowsour

Short communication

A facile nitridation method to improve the rate capability of TiO_2 for lithium-ion batteries

Mojtaba Samiee, Jian Luo*

Department of NanoEngineering, Program of Materials Science and Engineering, University of California, San Diego, La Jolla, CA 92093, USA

HIGHLIGHTS

- We report a facile method to significantly improve the rate capabilities of TiO_2.
- Capacities at 25C are significantly better than those reported in prior comparable studies.
- Lower nitridation temperatures result in moderate surface nitridation.
- Less-disordered nitridated surfaces increase conductivity w/o blocking Li transport.
- A simple and general approach to improve battery performances is suggested.

ARTICLE INFO

Article history:
Received 16 April 2013
Received in revised form
13 June 2013
Accepted 18 June 2013
Available online 10 July 2013

Keywords:
Lithium ion battery
TiO_2
Anode
Rate capability
Surface modification
Nitridation

ABSTRACT

It is demonstrated that the rate capacities of TiO_2 anatase nanoparticles can be improved substantially by annealing in NH_3 at 450–500 °C. At a high nominal rate of 25C, the average discharge capacity of specimens annealed in NH_3 at 450 °C for 7 h is more than double of that of the controlled specimens annealed in dry air under the same heat treatment condition. A critical comparison with literature shows that this simple and cost-effective low-temperature nitridation process can achieve high-rate capacities that are better than those reported in prior comparable studies. The enhanced high-rate capacities are attributed to moderate surface nitridation with less-disordered nitridated regions, which may enhance the surface electronic conductivity without forming discrete, nanoscale, surface amorphous films to block the lithium transport. Surface nitridation was confirmed by XPS measurements.

1. Introduction

A series of recent studies [1–3] demonstrated that the formation of oxide-based, nanometer-thick, surface amorphous films (SAFs) can enhance the rate capabilities of lithium-ion battery materials. As a unique high-temperature nanoscale wetting phenomenon, such SAFs can form spontaneously upon thermal annealing (driven by reduction of surface energies) with a self-selecting or "equilibrium" thickness on the order of 1 nm (in response to a balance of attractive and repulsive interfacial forces acting across the films) [3,4]; alternatively, these SAFs can be considered as a discrete nanoscale "surface phase" (also called "complexion" [5]) in the prewetting region [4]. In a similar effort, Liu et al. annealed V_2O_5 xerogel electrodes in N_2 to form surface defects (which can be considered as another type of surface "complexion") to enhance the battery performance [6]. The assembly of these recent studies points us to a new direction of improving the rate capabilities of lithium-ion battery materials via facile thermal treatments with controlled doping or in controlled chemical environments, which is enabled by spontaneously-occurred surface modifications that are driven by surface thermodynamics.

TiO_2 has been studied extensively as an anode material for lithium-ion batteries due to its high abundance and nontoxicity. However, TiO_2 has intrinsically low Li ion diffusivity and electronic conductivity, which hinder reversible lithiation capacities, particularly at high-rates; the electrochemical properties of anatase have been extensively studied and documented in Refs. [7–9]. In 2008, Park et al. reported that thermal nitridation of $Li_4Ti_5O_{12}$ in NH_3 can enhance its rate capabilities via formation of nanoscale, conductive, TiN based amorphous layers (which are likely to be TiO_xN_y in

* Corresponding author.
E-mail address: jluo@alum.mit.edu (J. Luo).

0378-7753/$ – see front matter © 2013 Elsevier B.V. All rights reserved.
http://dx.doi.org/10.1016/j.jpowsour.2013.06.113

reality) on the surfaces [10], and such layers exhibit similar character to those oxide-based SAFs [1–4]. In 2008, Han et al. showed that a nitrogen plasma treatment can enhance the discharge capacity of TiO_2 nanotubes [11]. In 2011, Han et al. further reported that nitridation of TiO_2 hollow nanofibers via annealing in a NH_3 gas atmosphere at 600 °C enhanced the rate capacity via forming similar TiN (TiO_xN_y) based SAFs [12]. TiN-based SAFs are expected to have high electronic conductivity to improve the rate capability of TiO_2, but TiN is electrochemically inactive with Li; consequently, the formation of relatively thick, discrete, and disordered TiN-based surface complexion may block Li transport. Thus, the surface nitridation process has to be optimized, which have not been conducted before. In this article, we use "nitridation" to refer to the formation of (titanium) nitride or oxynitride during annealing in ammonia gas atmosphere. We should note that TiN based surface "amorphous" films forming by nitridation of TiO_2 are likely to be oxynitride (TiO_xN_y) instead of pure TiN.

In this study, a systematic approach was used to investigate the effect of nitridation of TiO_2 nanoparticles via annealing in NH_3 at different temperatures and durations on the Li ion insertion properties; we also conducted comparative annealing in dry air under the same conditions. This study suggests that annealing at lower temperatures of 450–500 °C in NH_3 (as compared to the 600–650 °C annealing used in prior studies [10,12]) can produce moderate surface nitridation (with less surface structural disorder) without formation of discrete, nanoscale, TiN-based SAFs, which likely enhance electronic conductivity without blocking the lithium transport. Consequently, this study achieved the discharging capacities at ~25C that are better than those reported in prior studies [12–17] via a simple and cost-effective nitridation procedure.

2. Experimental procedure

TiO_2 anatase powders (~10 nm) were purchased from MTI Corporation (Richmond, CA). During the thermal annealing, TiO_2 nanoparticles were loaded into alumina combustion boats, which were placed in a tube furnace flowing a controlled gas (Ar, dry air or NH_3). Before each annealing, the tube furnace was flowed with high-purity Ar for 1 h to remove the air and moisture. In a typical thermal treatment, the temperature was raised from the room temperature to 250 °C at a rate of 7.5 °C min^{-1}, hold for 1 h at 250 °C (to remove moisture in the specimens), and raised at a heating rate of 5 °C min^{-1} to the desired (final) isothermal annealing temperature. Isothermal annealing temperatures of 450, 500 and 550 °C, respectively, were used in this study. Once reaching the final isothermal annealing temperature, the flowing gas was switched to NH_3. Specimens are also annealed in dry air for comparison. The final isothermal annealing duration was selected to be 1, 7 or 21 h. After the annealing was completed, the specimens were allowed to cool down under flowing Ar inside the tube furnace with power shut off.

The phase and crystallite size of the samples were evaluated by X-ray diffraction (XRD) using a Rigaku Ultima IV diffractometer with Cu K_α radiation ($K_{\alpha1}$ = 1.54056 Å), operating at 40 kV and 40 mA. X-ray photoelectron spectroscopy (XPS) measurements were carried out using a Kratos AXIS ULTRA^{DLD} XPS system equipped with an Al K_α monochromated X-ray source and a 165-mm electron energy hemispherical analyzer. Vacuum pressure was kept at $<3 \times 10^{-9}$ torr during the measurements. Particle surfaces were characterized using high-resolution transmission electron microscopy (HRTEM) using a Hitachi 9500 microscope operating at 300 kV. HRTEM specimens were prepared by dispersing particles ultrasonically in isopropanol, placing a small amount of suspension onto holey carbon-coated Cu grids and letting dry.

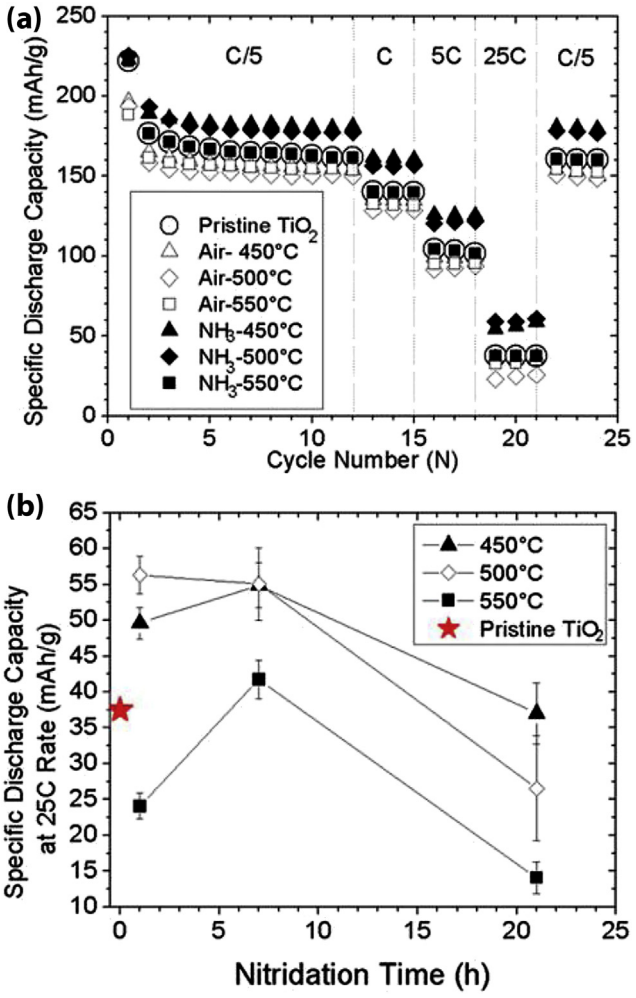

Fig. 1. (a) Comparison of rate performances of pristine TiO_2 and TiO_2 annealed in dry air and NH_3 at 450 °C, 500 °C and 550 °C, respectively, for 7 h. Discharge rates are labeled in the graph. (b) Effects of nitridation annealing time on specific discharge capacity at the 25C discharge rate for three sets of TiO_2 specimens annealed in NH_3 at 450 °C, 500 °C and 550 °C, respectively. In panel (b), each datum point represents the average of measurements of multiple specimens and the error bars are standard deviations.

Electrochemical properties of TiO_2 nanopowders were evaluated using coin cells assembled in an Ar-filled glovebox. To prepare working electrodes, a homogeneous mixture of active material, carbon black (99.9%; Alfa Aesar), and solution of Poly (vinylidene fluoride) (PVDF) (Sigma–Aldrich) in N-methyl-2-pyrrolidone (NMP) as the binder (Alfa Aesar), at a weight ratio of 80:10:10, was used. The mixture was uniformly pasted on Cu-foil (0.025 mm thick, 99.9%, Nimrod Hall), followed by overnight drying at 120 °C in vacuum. Pure lithium metal discs (Sigma–Aldrich) were used as counter electrodes, and Celgard C480 membranes were used as separators. A liquid electrolyte of 1 M $LiPF_6$ in ethylene carbonate (EC)/dimethyl carbonate (DMC)/diethyl carbonate (DEC) (1:1:1, by volume; MTI Corporation) was used. Electrochemical lithium insertion/extraction reactions were performed by an Arbin tester at different discharge rates, while all charge cycles were performed at C/5 rate. Details of coin cell construction and testing procedure can be found elsewhere [18]. A nominal rate of 1C denotes an insertion/extraction of 1 Li in 1 h with respect to the theoretical capacity of 330 mAh g^{-1} (noting that some researchers used the best achievable capacity to calculate C-rates in literature, which gave higher nominal C-rates).

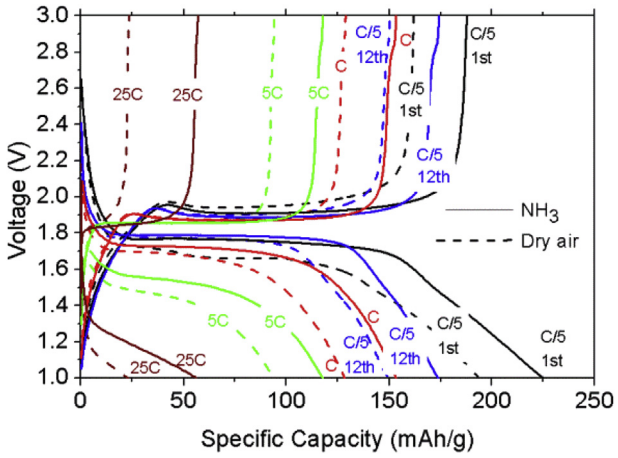

Fig. 2. Selected galvanostatic charge/discharge profiles of TiO_2 annealed at 500 °C for 7 h in dry air (dash lines) and NH_3 (solid lines) at different current densities.

3. Results and discussion

A comparison of the rate performances of pristine (as-received) and various annealed TiO_2 powders at discharge rates of C/5, C, 5C, 25C and C/5 in a sequence is shown in Fig. 1(a). Comparing with pristine TiO_2, annealing in NH_3 at 450 and 500 °C for 7 h substantially increases the discharging capacities at all rates. Specifically, the average discharge capacity is increased by 8–10% at C/5, 10–15% at 1C, ~20% at 5C, and ~45% at 25C. At the highest tested rate of 25C, the average discharge capacity is increased from ~38 mAh g^{-1} for pristine TiO_2 to ~55 mAh g^{-1} after annealing in NH_3 at 500 °C for 7 h, which is ~120% greater than the average capacity (~25 mAh g^{-1}) of the controlled specimens annealed in dry air at the same condition (Fig. 1a). Since we calculate the nominal C-rate with respect to the theoretical capacity of 330 mAh g^{-1}, the discharge capacity of ~55 mAh g^{-1} at the nominal 25C rate represents a full discharge in ~24 s (=1/25h × 55 mAh g^{-1}/330 mAh g^{-1}).

To systematically investigate the effect of nitridation temperature and duration, the averaged measured specific discharging capacities at 25C are plotted against nitridation time in Fig. 1(b) for three different annealing temperatures. For annealing at 450 °C, the discharge capacity increases with increasing the nitridation time from 1 h to 7 h, and then decreases with further increasing the nitridation time to 21 h. For annealing at 500 °C, the discharge capacity decreases slightly with increasing the nitridation time from 1 h to 7 h, and then more substantially with longer annealing of 21 h. The discharge capacity *vs.* nitridation time curve at 550 °C shows a similar trend to that at 450 °C, but with substantially lower capacities.

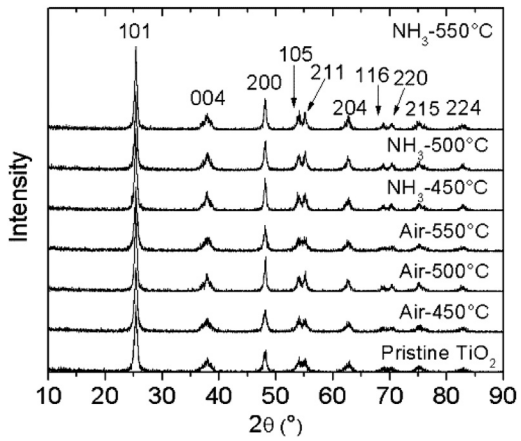

Fig. 3. XRD patterns of pristine and annealed TiO_2. All specimens (except for pristine TiO_2) shown here were annealed for 7 h, and the specific annealing temperature and atmosphere for each specimen are labeled in the graph.

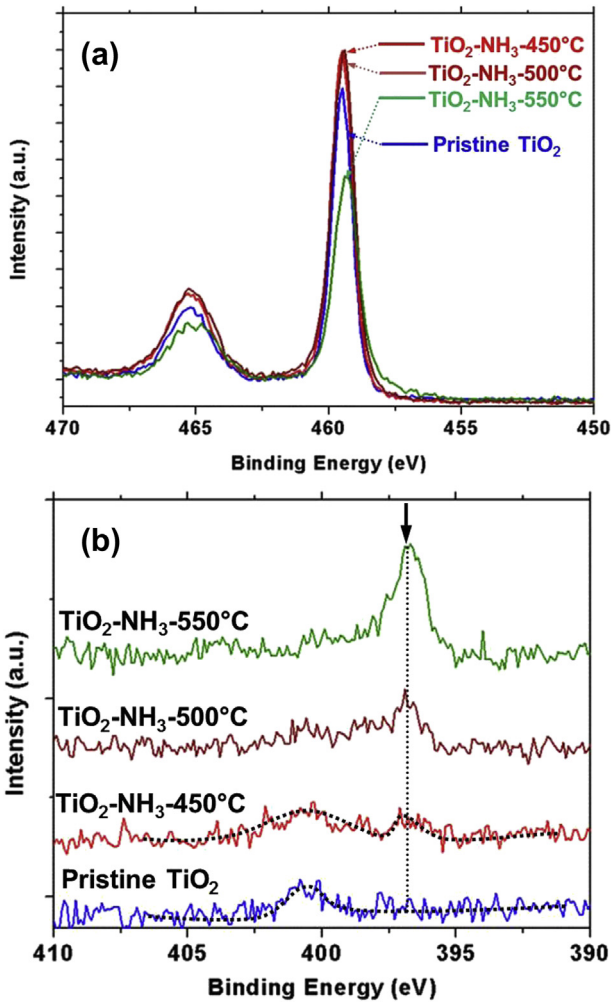

Fig. 4. (a) Ti 2p and (b) N 1s XPS spectra of the pristine and nitridated TiO_2. Nitridated TiO_2 powders were annealed in NH_3 at different temperatures for 7 h.

As a benchmark, TiO_2 nanoparticles were annealed in NH_3 and dry air in the same conditions (at 400, 450 and 550 °C, respectively) for comparison (Fig. 1a). Unlike annealing in NH_3, annealing in dry air decreases the discharging capacities slightly at all rates. A recent study [19] showed that annealing in air increased the capacity due to the increased crystallinity. However, in this case, the as-received TiO_2 nanoparticles already have high crystallinity and excellent reversible capacity of ~170 mAh g^{-1} at the rate of C/5; thus, further annealing in dry air did not further improve the capacity.

The discharging capacities at high-rates (at ~25C nominal rate) achieved in this study via a simple nitridation treatment at the optimal heat treatment conditions (450 °C, 7 h or 500 °C, 1 h) are better than those reported in prior studies [12–17]; most notably, these include nitridated TiO_2 hollow nanofibers with specially-designed complex geometry to maximally enhance transport and more fabrication steps; the capacity of those nitridated TiO_2 hollow nanofibers is ~25 mAh g^{-1} at 10C, while this study achieved ~55 mAh g^{-1} (>2×) at an even higher rate 25C (2.5×) [12]. This discharge capacity of ~55 mAh g^{-1} at 25C is also better than the

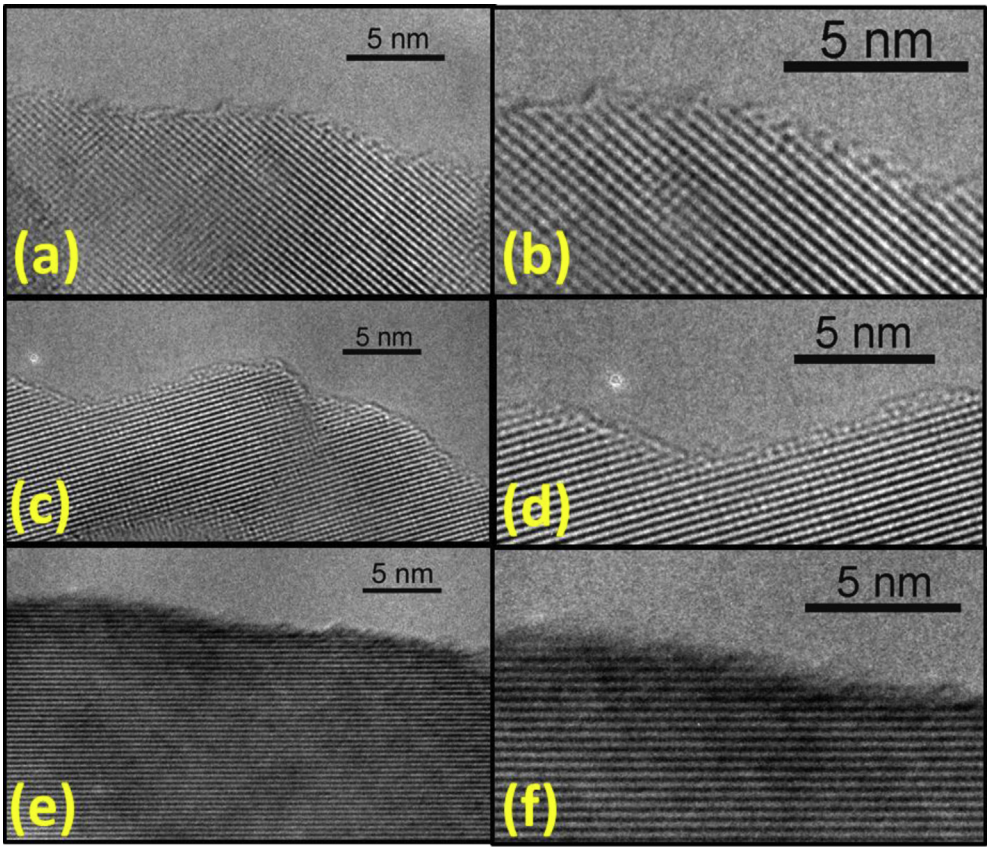

Fig. 5. Representative HRTEM micrographs of surfaces of TiO_2 nanoparticles annealed at (a,b) 450 °C in air, (c,d) 450 °C in NH_3 and (e,f) 550 °C in NH_3, respectively, for 7 h.

best achieved result of TiO_2 nanoparticles treated in H_2 (~40 mAh g^{-1} at 20C) [13]. After conducting a comprehensive literature survey and analysis, we found that this rate performance at ~25C is better than those achieved in comparable prior studies, including TiO_2/carbon composites with high carbon loadings and smaller particles size [14], carbon coated TiO_2 using sucrose [15], Pt doped TiO_2 with a much smaller particle size of 4 nm [16], and TiO_2 nanotube/carbon composites [17].

The only better reported results for the discharge capacity at similar C-rates in literature were achieved by two substantially-more-complex hierarchical composites: a "hierarchical mesoporous TiO_2:RuO_2 composite" with "efficient hierarchical mixed conducting networks" [20] and an "ultrathin TiO_2 nanotube/C" composite with smaller size (~3.5 nm inner diameter) [21], for which direct comparisons are probably not feasible (nor fair). It is interesting to note that the performance reported here is better than their "non-composite" controlled specimens in those two reports [20,21], *i.e.*, comparable discharge capacities at 20–30C were reported in Ref. [20] for 5-nm TiO_2 nanoparticles with high carbon loadings and in Ref. [21] with ultrathin TiO_2 nanotubes (the effective performance reported here is considered better because TiO_2 with smaller dimensions were used in those studies). Synthesis of complex composite electrodes is presumably more expensive.

Representative galvanostatic discharge/charge curves of TiO_2 powders annealed in dry air and NH_3 at 500 °C at different current densities are shown in Fig. 2. Both sets of specimens show typical electrochemical characteristics of anatase TiO_2, exhibiting cathodic insertion of lithium at ~1.75 V and anodic extraction of lithium at ~1.95 V *vs.* Li/Li^+, which indicates the same charge/discharge mechanism. A close look at charge/discharge curves reveals that the potential separation between anodic extraction and cathodic insertion plateau is less for nitridated TiO_2 in comparison with TiO_2 annealed in dry air, which indicates better reversibility of Li^+ insertion and extraction in nitridated TiO_2. By increasing the current densities (to 5C and 25C), the capacity contributed by the plateau part decreases, indicating possible surface Li storages.

It was reported that the conversion reaction of electrospun anatase fibers to TiO_xN_y starts at about 550 °C [22]. Our XRD analysis showed that the TiO_2 powders annealed in air and ammonia between 450 and 550 °C are all phase-pure anatase, and there is no observable secondary phases by XRD (Fig. 3); this is in agreement with previous reports that nitridation at temperatures lower than 550 °C does not change the crystal structure of anatase TiO_2 [12]. Particles sizes for pristine TiO_2 and six treated TiO_2 (which were annealed in air and NH_3, respectively, at 450, 500 and 550 °C, respectively) were determined to be 9–11 nm from peak broadening of X-ray diffraction using the Scherrer Equation. We measured the crystallite sizes for each of the seven specimen using both (101) and (200) peaks, and results are always consistent with <10% relative errors in all seven cases. Thus, we conclude that there is no significant coarsening (that is observable with the typical XRD measurement errors) in all thermally treated nanoparticles.

Considering there is no observable difference in the crystallite size for TiO_2 nitridated at 450–500 °C, it is interesting to note that TiO_2 nitridated at 550 °C has significantly lower capacities. A similar phenomenon (of decreasing activity for annealing in NH_3) was observed for the visible-light activity of nitridated TiO_2 [23], which was attributed to a change of the chemical state of N dopants in TiO_2 with increased concentration of Ti^{3+} in the surface and bulk of TiO_2 particles [23]; prior reports showing that excessive concentration of Ti^{3+} decreases the discharge capacity of TiO_2

nanoparticles via decreasing the concentration of Li^+ ions [13,24], which may explain the reduced capacities after nitridation at 550 °C.

The chemical states of titanium and nitrogen were characterized by XPS. As shown in Fig. 4(a), the Ti $2p_{3/2}$ peak for the pristine TiO_2 shows a symmetric shape and the binding energy centered at 458.2 eV, which corresponds to Ti^{4+} in the tetragonal structure of stoichiometric TiO_2. For nitridated TiO_2 powders, this peak becomes asymmetric and shifts to lower binding energies. By increasing the nitridation temperature to 550 °C, a new and weak Ti $2p_{3/2}$ core level peak appears as a side lump at 457.5 eV. This peak represents titanium species with oxidation sates between +3 and +4, which is correlated with titanium in a distorted lattice located between TiO_2 and TiN.

The measured N 1s XPS spectra, which are shown in Fig. 4(b), provide more convincing evidence for surface nitridation. There is only one N 1s peak for pristine TiO_2 at about 401 eV, which can be assigned to molecular nitrogen adsorbed on surfaces [25]. For the powder nitridated at 450 °C, another weak peak appears at about 396.5 eV (labeled by the arrow and dashed line in Fig. 4b), which can be assigned to atomic state of nitrogen bonded to three Ti atoms (N^{3-} species) since the binding energy is close to that of TiN (396.0 eV) [25]. The intensity of this N^{3-} peak increases by increasing the nitridation temperature (Fig. 4b). These XPS results clearly indicate the occurrence of surface nitridation (forming of TiO_xN_y) for specimens annealed in NH_3 between 450 and 550 °C.

Prior studies showed that annealing TiO_2 nanotubes [12], as well as $Li_4Ti_5O_{12}$ particles [10], in NH_3 at 600 and 650 °C results in the formation of nanometer-thick, amorphous layers or SAFs of TiN/TiO_xN_y on the surfaces, which exhibit good electronic conductivity to enhance the rate capabilities (but are electrochemically inactive with lithium). HRTEM characterization showed that such discrete and disordered SAFs were not observed for TiO_2 nanoparticles nitridated at a lower temperature 450 °C for 7 h (Fig. 5c,d), while the surfaces of nanoparticles nitridated at 550 °C for 7 h exhibit a low level of disorder (Fig. 5e,f); the surfaces exhibit some similar disorder character to those nanoscale SAFs of TiN/TiO_xN_y observed TiO_2 nanotubes [12] and $Li_4Ti_5O_{12}$ nitridated at 600 and 650 °C, but with thinner effective thickness and less-disordered surface structures. Consequently, it is reasonable to attribute the increased rate capability of TiO_2 annealed at 450–500 °C in NH_3 (achieved in this study) to some more moderate surface nitridation, which was verified by XPS (Fig. 4); but the lower nitridation temperatures result in thinner surface nitridation region and less structural disorder in comparison with the TiN/TiO_xN_y SAFs formed after nitridation at 600 and 650 °C [10,12]; it is known that various nitrogen species can form on the surfaces of TiO_2 nanoparticles via nitridation [23]. Although these surface nitridation regions formed at lower temperatures of 450–500 °C are more ordered and thinner than the discrete amorphous layers or SAFs of TiN/TiO_xN_y formed 600 °C, it should still enhance the surface electronic conductivity; a better result achieved by this study (as comparing with those TiO_2 nanotubes nitridated at 600–650 °C [12]) may be related to thinner and less-disordered surface nitridation regions (Fig. 5) that do not block Li^+ transport.

4. Conclusions

We have systematically investigated the effect of nitridation temperature and time on the electrochemical properties of anatase TiO_2. Annealing in NH_3 at 450–500 °C increases the discharge capacities of TiO_2 nanoparticles substantially. Via this simple and cost-effective nitridation treatment, this study achieved the discharging capacities at ~25C that are better than those reported in prior studies [12–17]. This study suggested that lower nitridation temperatures of 450–500 °C for annealing in NH_3 (as compared to the typical 600–650 °C annealing used in prior studies) can lead to better results, which are attributed to more moderate surface nitridation with thinner and less-disordered nitridated regions that enhance electronic conductivity without blocking lithium transport.

In a broad context, this work, along with a number of recent studies [1–3,6], suggests a generally-useful facile method to improve rate capabilities of battery materials via thermal treatments with controlled doping or in controlled atmospheres to achieve spontaneously-occurred surface modifications driven by surface thermodynamics (via the formation of surface "phase" or complexion). This method may also be applied to improve a variety of other properties, *e.g.*, it was demonstrated that disordered surface complexion formed in TiO_2 anatase can also be utilized to improve photocatalytic activities [26,27].

Acknowledgment

This work is financially supported by an NSF grant no. DMR-1006515 in the Ceramics program, managed by Dr. Lynnette D. Madsen. The authors thank Prof. Zaera and Dr. Lee at UC Riverside for XPS measurements with equipment supported by an NSF grant no. DMR-0958796.

References

[1] B. Kang, G. Ceder, Nature 458 (2009) 190–193.
[2] K. Sun, S.J. Dillon, Electrochem. Commun. 13 (2011) 200–202.
[3] A. Kayyar, H.J. Qian, J. Luo, Appl. Phys. Lett. 95 (2009) 221905.
[4] J. Luo, Y.-M. Chiang, Annu. Rev. Mater. Res. 38 (2008) 227–249.
[5] M.P. Harmer, Science 332 (2011) 182–183.
[6] D.W. Liu, Y.Y. Liu, A.Q. Pan, K.P. Nagle, G.T. Seidler, Y.H. Jeong, G.Z. Cao, J. Phys. Chem. C 115 (2011) 4959–4965.
[7] T. Froschl, U. Hormann, P. Kubiak, G. Kucerova, M. Pfanzelt, C.K. Weiss, R.J. Behm, N. Husing, U. Kaiser, K. Landfester, M. Wohlfahrt-Mehrens, Chem. Soc. Rev. 41 (2012) 5313–5360.
[8] T. Berger, D. Monllor-Satoca, M. Jankulovska, T. Lana-Villarreal, R. Gomez, ChemPhysChem 13 (2012) 2824–2875.
[9] L. Kavan, Chem. Rec. 12 (2012) 131–142.
[10] K.-S. Park, A. Benayad, D.-J. Kang, S.-G. Doo, J. Am. Chem. Soc. 130 (2008) 14930–14931.
[11] K.S. Han, J.W. Lee, Y.M. Kang, J.Y. Lee, J.K. Kang, Small 4 (2008) 1682–1686.
[12] H. Han, T. Song, J.-Y. Bae, L.F. Nazar, H. Kim, U. Paik, Energy Environ. Sci. 4 (2011) 4532–4536.
[13] J.-Y. Shin, J.H. Joo, D. Samuelis, J. Maier, Chem. Mater. 24 (2012) 543–551.
[14] J. Lee, Y.S. Jung, S.C. Warren, M. Kamperman, S.M. Oh, F.J. DiSalvo, U. Wiesner, Macromol. Chem. Phys. 212 (2011) 383–390.
[15] S.K. Das, M. Patel, A.J. Bhattacharyya, ACS Appl. Mater. Interf. 2 (2010) 2091–2099.
[16] P. Singh, M. Patel, A. Gupta, A.J. Bhattacharyya, M.S. Hegde, J. Electrochem. Soc. 159 (2012) A1189–A1197.
[17] S. Yoon, B.H. Ka, C. Lee, M. Park, S.M. Oh, Electrochem. Solid State Lett. 12 (2009) A28–A32.
[18] A. Kayyar, J. Huang, M. Samiee, J. Luo, J. Visual Exp. (2012) e4104.
[19] J.W. Kang, D.H. Kim, V. Mathew, J.S. Lim, J.H. Gim, J. Kimz, J. Electrochem. Soc. 158 (2011) A59–A62.
[20] Y.-G. Guo, Y.-S. Hu, W. Sigle, J. Maier, Adv. Mater. 19 (2007) 2087–2091.
[21] J. Zhang, X. Yan, J. Zhang, W. Cai, Z. Wu, Z. Zhang, J. Power Sources 198 (2012) 223–228.
[22] M. Zukalova, J. Prochazka, Z. Bastl, J. Duchoslav, L. Rubacek, D. Havlicek, L. Kavan, Chem. Mater. 22 (2010) 4045–4055.
[23] Z. Zhang, X. Wang, J. Long, Q. Gu, Z. Ding, X. Fu, J. Catal. 276 (2010) 201–214.
[24] J.-Y. Shin, D. Samuelis, J. Maier, Solid State Ionics 225 (2012) 590–593.
[25] R. Asahi, T. Morikawa, T. Ohwaki, K. Aoki, Y. Taga, Science 293 (2001) 269–271.
[26] X.B. Chen, L. Liu, P.Y. Yu, S.S. Mao, Science 331 (2011) 746–750.
[27] M. Samiee, J. Luo, Mater. Lett. 98 (2013) 205–208.